Cooling a Magnetic Nanoisland by Spin-Polarized Currents

J. Brüggemann,[1] S. Weiss,[2] P. Nalbach,[1] and M. Thorwart[1]
[1]*I. Institut für Theoretische Physik, Universität Hamburg, Jungiusstraße 9, 20355 Hamburg, Germany*
[2]*Theoretische Physik, Universität Duisburg-Essen and CENIDE, 47048 Duisburg, Germany*
(Received 22 January 2014; revised manuscript received 19 May 2014; published 14 August 2014)

We investigate cooling of a vibrational mode of a magnetic quantum dot by a spin-polarized tunneling charge current exploiting the magnetomechanical coupling. The spin-polarized current polarizes the magnetic nanoisland, thereby lowering its magnetic energy. At the same time, Ohmic heating increases the vibrational energy. A small magnetomechanical coupling then permits us to remove energy from the vibrational motion and cooling is possible. We find a reduction of the vibrational energy below 50% of its equilibrium value. The lowest vibration temperature is achieved for a weak electron-vibration coupling and a comparable magnetomechanical coupling. The cooling rate increases at first with the magnetomechanical coupling and then saturates.

DOI: 10.1103/PhysRevLett.113.076602 PACS numbers: 72.25.-b, 73.63.-b, 75.76.+j, 85.80.-b

The ongoing miniaturization of electronic devices will sooner or later have to face the problem of how to efficiently remove inevitable heating from the devices. Up to now, essentially all electronic devices operate on the basis of dumping heat via passive sinks via the supporting structure. Active or dynamical nanocooling has received little attention, although passive thermal transport is inefficient at the nanoscale. In addition, most present nanoelectronic or -magnetic devices function at low temperatures only. Efficient applications will, thus, demand dynamic nanorefrigerators. Nanocooling would also facilitate new experiments which are not conceivable today due to the spacious equipment required for cooling.

Various forms of nanorefrigerators in which heat is carried by an electronic charge current have been proposed [1]. We, in contrast, propose to use the electronic spin for cooling, similar to the macroscale magnetocaloric demagnetization cooling [2]. Typically, cooling requires the opening and closing of heat links which is realized at the macroscale by mechanically moving parts or using coolants. This is impractical at the nanoscale. Instead, we propose using spin-polarized currents to polarize a magnetic nanoisland, thereby lowering its magnetic energy. Subsequent energy exchange due to a magnetomechanical coupling between the magnetic and vibrational degrees of freedom can then reduce the vibrational energy. Electric losses give rise to Ohmic heating. Thus, a net cooling is reached when the polarization of the magnetic moment is faster than Ohmic heating.

In detail, we investigate the nonequilibrium quantum dynamics of a magnetic quantum dot with a single electronic level, a local magnetic moment $\boldsymbol{J}$, and a single vibrational mode as sketched in Fig. 1. The magnetic quantum dot is weakly coupled to ferromagnetic spin-polarized electronic leads via tunneling. Charge and spin currents through quantum dots with an additional magnetic moment or an additional vibrational mode have been studied extensively [3–10], but the full model including both has been unexplored so far. For weak tunneling contacts, the sequential tunneling processes dominate, and a description by classical or quantum master equations is adequate [11,12]. Spin-polarized currents can polarize the local magnetic moment $\boldsymbol{J}$ against an applied magnetic field and, thus, can lower its energy. At the same time, the vibrational motion is heated due to Ohmic losses. The final goal is to cool the vibrational mode by means of an effective magnetomechanical coupling which allows for an energy exchange between the local magnetic moment $\boldsymbol{J}$ and the vibrational mode. Such magnetomechanical couplings have been suggested theoretically for a nanomechanical cantilever which interacts with a ferromagnetic tip on its surface [13], for a nitrogen-vacancy (NV) impurity in diamond which couples to the magnetic tip of a nanomechanical cantilever [14], for a magnetic nanoparticle or a single molecular magnet attached to a torsional doubly clamped resonator [15], and for a single electron spin which couples to a flexural mode of a suspended carbon nanotube [16]. The experimental detection of the coupling of an individual electron spin and the magnetic tip of a cantilever was successful [17]. Magnetomechanical coupling of a

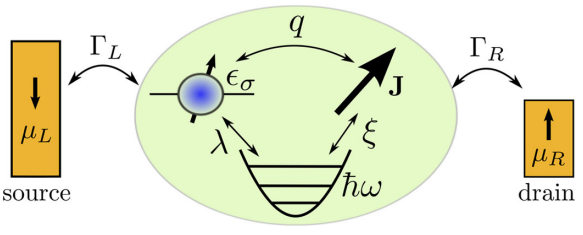

FIG. 1 (color online). Schematic consisting of ferromagnetic leads, a quantum dot with a localized magnetic moment, and a single vibrational mode.

single NV center to a SiC cantilever has also been demonstrated [18,19]. Furthermore, a strong coupling between the magnetic moment of a single molecular magnet and a suspended carbon nanotube has been reported [20]. This magnetomechanical coupling can be explored for cooling the vibrational motion. We provide an intuitive picture of the concept and determine viable parameters for the cooling of the vibration below its equilibrium temperature. The lowest vibrational energy is achieved for a weak electron-vibration coupling and a comparable magnetomechanical coupling.

Model.—Our minimal model is sketched in Fig. 1. The quantum dot is given as a single electronic level with energy ϵ_0. For small dots, the local charging energy exceeds all other energies, and a double dot occupancy is forbidden. The Hamiltonian is $H_d = \epsilon_0(a_\uparrow^\dagger a_\uparrow + a_\downarrow^\dagger a_\downarrow) + (g\mu_B/\hbar)Bs_z$, with electron operators a_σ and $a_\sigma^\dagger$, the g factor g, and the Bohr magneton μ_B. The spin projection quantum number is σ and s_z the z component of the electron spin $\boldsymbol{s} = (\hbar/2)\sum_{\sigma,\sigma'} a_\sigma^\dagger \boldsymbol{\sigma}_{\sigma\sigma'} a_{\sigma'}$. A small external field B splits the spin states along the quantization axis. The localized magnetic moment is modeled by a spin-1/2 impurity. Generalization to higher spin values is possible. We denote with $J_z = \pm\hbar/2$ the projection onto the quantization axis. The corresponding Hamiltonian is $H_J = (g\mu_B/\hbar)BJ_z + \frac{q}{\hbar^2}(\boldsymbol{s}\cdot\boldsymbol{J})$, where the electronic spin and the local magnetic moment $\boldsymbol{J}$ are coupled by an exchange interaction of strength q, for simplicity, assumed to be isotropic. To study the dynamical heating, a vibrational mode of frequency ω is coupled to the dot. Using bosonic ladder operators b and $b^\dagger$, we obtain $H_{ph} = \hbar\omega b^\dagger b + \lambda(b + b^\dagger)\sum_\sigma a_\sigma^\dagger a_\sigma$. The linear coupling of the electronic occupation to $(b + b^\dagger)$ allows us to excite or relax the vibrational mode by each tunneling electron. It also describes heating of the mode due to the charge current. The crucial ingredient is a magnetomechanical coupling between the magnetic moment $\boldsymbol{J}$ and the vibrational degree of freedom included by

$$H_{J-\mathrm{ph}} = \frac{\xi}{\hbar}(b + b^\dagger)(J_+ + J_-), \tag{1}$$

where $J_\pm = (J_x \pm iJ_y)/2$ are spin-1/2 ladder operators inducing transitions between the magnetic states when at the same time the vibrational mode changes its angular momentum state [21]. Experimental values for ξ and λ can readily be extracted for the existing experimental setups. Ganzhorn *et al.* [20] realized a setup with a single molecular magnet covalently bound to a carbon nanotube suspended between two leads. The molecule has a magnetic ground state of $|\boldsymbol{J}| = 6$ and the ground state doublet $J_z = \pm 6$ is separated from the excited states by several hundreds of kelvin. Hence, an Ising-like spin flip between these two states via quantum spin tunneling is dominant, and the physics is well described by an effective spin 1/2. The spin flip is accompanied by a transition in the vibrational mode, and one finds [20] $\omega = 34$ GHz, $\xi = 1.5$ MHz, and $\lambda = \omega\sqrt{g} = 26$ GHz for $g = 0.6$, implying that $\xi/\omega \sim 4 \times 10^{-5}$ and $\lambda/\omega \sim 0.76$. For the NV centers [18], we have $\omega = 2\pi \times 625$ kHz and $\xi = g\mu_B(\partial B/\partial z)\sqrt{\hbar/(2m\omega)} \sim 172$ Hz, implying that $\xi/\omega \sim 4 \times 10^{-6}$. Another realization [19] yields $\omega = 2\pi \times 80$ kHz and $\xi \sim 8$ Hz, such that $\xi/\omega \sim 10^{-4}$. The quantum dot is tunnel coupled to two ferromagnetic (FM) leads, whose magnetization directions are, in general, noncollinear. They are modeled as noninteracting electron reservoirs $H_{\mathrm{leads}} = \sum_{k\alpha}(\epsilon_{k\alpha} - \mu_\alpha)(c_{k\alpha+}^\dagger c_{k\alpha+} + c_{k\alpha-}^\dagger c_{k\alpha-})$, where $c_{k\alpha\pm}$ represents the annihilation operator for an electron with the wave number k and the majority or minority spin in the lead $\alpha = L$, R and $\mu_{L/R} = \pm eV/2$ is the chemical potential of the leads shifted by the applied bias voltage V. In the FM leads, the spin species have different density of states at the Fermi energy. We define the polarization $p_\alpha = (\nu_{\alpha,+} - \nu_{\alpha,-})/(\nu_{\alpha,+} + \nu_{\alpha,-})$ of lead α by the relative difference in the density of states $\nu_{\alpha,\pm}$ for majority or minority spins at the Fermi energy. We use $p_L = p_R = p$. All energies are measured relative to the Fermi energy at zero polarization. Spin dynamical effects, which affect the vibrational dynamics, are influenced by the relative angle between the magnetization directions of the leads due to the exchange field on the dot [3]. The source lead polarization is chosen as antiparallel to B. We consider three setups with drain polarization parallel ($\downarrow\downarrow$), perpendicular ($\downarrow\rightarrow$), or antiparallel ($\downarrow\uparrow$) to the source. To have an overall quantization axis, the tunneling Hamiltonian depends explicitly on spin rotation matrices as $H_t = \sum_{k,\alpha=L/R}[t_{k\alpha}A_\mu \Lambda_{\mu\nu}^{(\alpha)} C_{\nu;k,\alpha}^\dagger + \mathrm{H.c.}]$ with $A = (a_\uparrow, a_\downarrow)$, $C_{k,\alpha} = (c_{k\alpha+}, c_{k\alpha-})$, and $\Lambda^{(L)} = \Lambda^{(R,\mathrm{para})} = \mathbb{1}$, $\Lambda^{(R,\mathrm{anti})} = \sigma_x$, and $\Lambda^{(R,\mathrm{perp})} = (\mathbb{1} - i\sigma_y)/\sqrt{2}$ for the three setups. The hybridization with the dot state in the wideband limit is given by $\Gamma_\alpha = 2\pi|t_{k\alpha}|^2(\nu_{\alpha,+} + \nu_{\alpha,-})$.

Method.—Spin polarization and excitations of the vibration are explicit dynamical processes while the lead electrons can be integrated out. The time evolution of the reduced density matrix includes the dot electrons, the magnetization, and the vibration and obeys the kinetic equation [11,12]

$$\partial_t \rho_{\chi_2}^{\chi_1}(t) = -i(\epsilon_{\chi_1} - \epsilon_{\chi_2})\rho_{\chi_2}^{\chi_1}(t) - \int_{t_0}^{t} dt' \sum_{\chi_1'\chi_2'} M_{\chi_2'\chi_2}^{\chi_1'\chi_1}(t,t')\rho_{\chi_2'}^{\chi_1'}(t'), \tag{2}$$

with ϵ_{χ_i} describing the system's eigenenergies. It includes all quantum coherences of the system as well as all nonequilibrium effects due to the leads. In practice, we diagonalize numerically the Hamiltonian of dimension $6n$ spanned by the states spin-up, spin-down, and empty for the dot electron level with spin-up or spin-down of the local magnetization. n is the number of vibrational states

necessary for convergence and depends on λ, T, and V. Here, $n = 6$ is sufficient. For small tunnel couplings $\Gamma_\alpha \ll (B, q, \lambda, k_B T)$, the tensor M can be expanded to lowest orders in Γ_α. Taking into account the finite bias voltage, this gives irreducible self-energies on the Keldysh contour [11,12]. The leads are held at temperature T.

In the Markov limit, we solve the kinetic equation and calculate the occupation probabilities for the subspaces of the dot, the local magnetic moment and vibration are by further tracing over the respective other degrees of freedom. Then, we monitor the spin polarization of the dot and population of vibrational states. The electron current follows by standard means [3].

Principle mechanism.—To provide a qualitative understanding, we start from an empty dot and the local magnetic moment $\boldsymbol{J}$ being aligned with the magnetic field, say, pointing upwards, i.e., being in the high-energy state. The vibrational degree of freedom is assumed to be in a thermal state at the lead temperature T. A source lead perfectly polarized down enforces all electrons tunneling into the quantum dot to have spin-down. The tunneling of a single spin-down electron onto the dot lowers the dot energy because of the $\boldsymbol{s} \cdot \boldsymbol{J}$-exchange coupling. Because of the FM leads together with the local magnetic field, the electron spin and the localized magnetic moment are not conserved. This permits a spin flip of the electron spin upwards and the local moment downwards. This lowers the energy of the local magnetization which is transferred to the electron. If the drain is polarized antiparallel to the source, i.e., upwards, the electron can tunnel preferably out of the dot only after its spin has flipped. Thus, antiparallel polarized leads ensure spin flips and, thus, lower the total current. Any electronic population of the dot generates vibrational transitions due to the electron-vibration coupling λ. At finite bias voltage, this generates Ohmic heating of the vibration above the lead temperature. In turn, the magneto-mechanical coupling ξ now provides a possibility for an energy exchange between the magnetization and the vibration. In particular, the vibration can relax while the magnetization is flipped upwards and, thus, parallel to the magnetic field again, which reflects its high-energy state. The next spin-down electron, which tunnels into the quantum dot, will remove this energy, and a net cooling of the vibrational motion results. Nonperfect lead polarizations will lower the cooling efficiency since not every electron spin will be forced to flip.

Results.—To confirm this qualitative picture, we show in Fig. 2(a) the time evolution of the local magnetization $\langle J_z \rangle$ for the parallel ($\downarrow\downarrow$), the perpendicular ($\downarrow \rightarrow$), and the antiparallel ($\downarrow\uparrow$) lead polarizations. The system is initialized by allowing equilibration with the leads at $V = 0$. A Boltzmann distribution defines an initial temperature $T_{\rm init} = \langle H_{\rm ph}(t = 0) \rangle / k_B$ of the equilibrated vibration before applying a bias voltage. For ($\downarrow\downarrow$) alignment, electrons with majority spin can tunnel through the quantum dot without flipping the spin. No spin blockade occurs, and the steady state with a large charge current is reached on a time scale of Γ^{-1} [see Fig. 2(b)]. The energy of the vibrational mode, i.e., $\langle H_{\rm ph} \rangle / \epsilon_0$, increases slightly; see Fig. 2(c). Subsequently, due to the weak coupling between the vibration and $\boldsymbol{J}$, a slow decrease of the polarization $\langle J_z \rangle / \hbar$ follows; see Fig. 2(a).

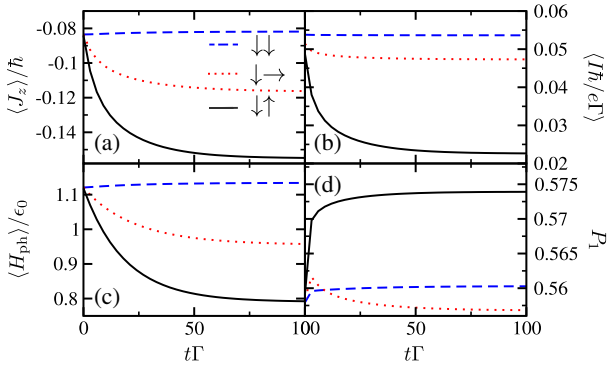

FIG. 2 (color online). (a) Polarization $\langle J_z \rangle / \hbar$ of the localized magnetic moment along the z direction, (b) charge current $\langle I\hbar/e\Gamma \rangle$, (c) vibrational energy $\langle H_{\rm ph} \rangle / \epsilon_0$, and (d) probability P_1 to find one electron on the quantum dot as a function of time for the three different lead setups. The remaining parameters are $p = 0.9$, $\hbar\Gamma = 0.01\epsilon_0$, $B = 0.7\epsilon_0/(g\mu_B)$, $\hbar\omega = 0.75\epsilon_0$, $k_B T = 2\epsilon_0$, $q = 0.4\epsilon_0$, $\xi = 0.06\epsilon_0$, $\lambda = 0.2\epsilon_0$, and $eV = 1.2\epsilon_0$.

For the ($\downarrow \rightarrow$) alignment, the different spin carrier distributions in the leads cause a strong spin blockade which suppresses the current [see Fig. 2(b)] as compared to the ($\downarrow\downarrow$) case. At the same time, a sizeable electron spin accumulates on the dot. A partial polarization $\langle J_z \rangle / \hbar$ and cooling, i.e., a decrease of the vibrational energy, is observed. An optimal polarization of the local magnetic moment is, however, obtained for the ($\downarrow\uparrow$) alignment. Here, the minimal steady-state current and the lowest energy in the vibrational mode, the strongest cooling, is found. In

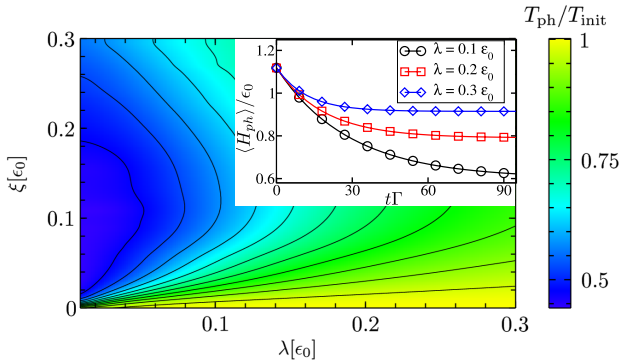

FIG. 3 (color online). Effective vibrational temperature $T_{\rm ph}$ in the stationary limit versus electron-vibration coupling λ and magnetization-vibration coupling ξ. Inset: Vibrational energy $\langle H_{\rm ph} \rangle$ versus time for different electron-vibration coupling strengths λ. The remaining parameters are as in Fig. 2.

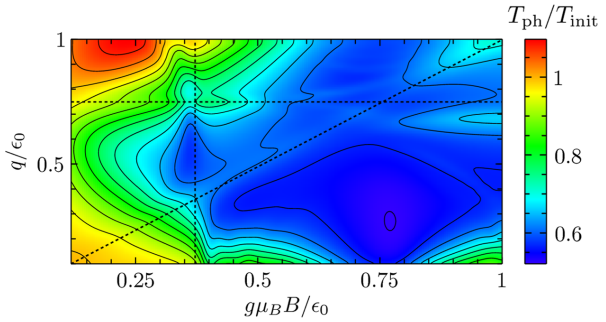

FIG. 4 (color online). Effective vibrational temperature T_{ph} in the stationary limit versus magnetic field $g\mu_B B$ and spin-magnetization coupling q. The used parameters are $\xi = 0.12\epsilon_0$, $\lambda = 0.1\epsilon_0$, with the remaining parameters as in Fig. 2.

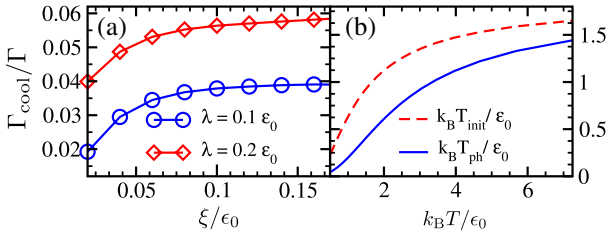

FIG. 5 (color online). (a) Vibrational cooling rate Γ_{cool} versus the magnetomechanical coupling ξ for two electron-vibration couplings $\lambda = 0.1\epsilon_0$ and $\lambda = 0.2\epsilon_0$. (b) Effective vibrational temperature in the initial, thermalized state (T_{init}, $V = 0$, red dashed line) and in the final steady state (T_{ph}, $V > 0$, blue solid line) as a function of the lead temperature T for $\xi = 0.12\epsilon_0$ and $\lambda = 0.1\epsilon_0$. The remaining parameters are as in Fig. 2.

Fig. 2(d), the dot occupation probability P_1 is shown as a function of time for all three setups. The finite charge accumulation for all lead polarizations combined with the different steady-state currents [see Fig. 2(b)] demonstrates the current blockade for the antiparallel setup. As expected, the $\downarrow\uparrow$ setup is shown to be optimal in two respects. First, it produces the largest magnetic polarization of the dot against an applied magnetic field and, thus, lowers the magnetic energy of $\boldsymbol{J}$ optimally. Second, the spin blockade suppresses the charge current and enforces that each transmitted electron can contribute to the polarization process and, thus, to cooling. Additionally, the Ohmic heating is directly connected to the charge current and, therefore, suppressed, which significantly improves the cooling efficiency.

We focus on weak-to-intermediate electron-vibration coupling where the vibrational blockade is absent. For $\xi = 0$, we observe for all setups an increasing energy $\langle H_{ph}\rangle/\epsilon_0$ of the vibrational mode with a stronger heating for a larger electron-vibration coupling. For a finite magnetomechanical coupling $\xi \neq 0$, energy is exchanged with the polarized or cooled local moment, and a net cooling of the vibrational mode results. In total, these results illustrate the proof of principle of cooling a magnetic nanodevice by a spin-polarized current.

In order to quantify the cooling, we define an effective vibrational temperature T_{ph} assuming a Boltzmann distribution in the steady state [22] as

$$T_{ph} = \langle H_{ph}\rangle_{stat}/k_B. \tag{3}$$

Figure 3 shows the ratio of T_{ph} and the initial temperature T_{init} as a function of the electron-vibration coupling λ and the magnetomechanical coupling ξ. Cooling is achieved in the full parameter regime depicted. As expected, with increasing electron-vibration coupling λ, the effective vibrational temperature increases (see inset of Fig. 3). Surprisingly, for fixed λ, we observe a nonmonotonic dependence of the cooling as a function of ξ (vertical cut in Fig. 3). At first, T_{ph} decreases with increasing ξ. However, a minimum is reached where cooling is optimal. For further increasing ξ, the effective vibrational temperature increases again. In Fig. 4, T_{ph} is shown as a function of the magnetic field $g\mu_B B$ and the spin-magnetization exchange coupling q. For higher magnetic fields, the cooling effect is increased since the energy gain due to the spin polarization is proportional to the magnetic field. Additional fine structures are observed and traced back to resonances between spin flips and vibrational transitions (see dashed lines in Fig. 4 for the noninteracting limit, ξ, $\lambda \to 0$). An effective temperature as in Eq. (3) can be defined at all times. We find an exponential approach to the steady state. Thus, we can determine the effective cooling rate Γ_{cool} by a fit to our numerical results according to $T_{ph}(t) \simeq T_{ph}(\infty) + e^{-\Gamma_{cool} t}[T_{init} - T_{ph}(\infty)]$. Figure 5(a) depicts the cooling rate versus the magnetomechanical coupling for two values of electron-vibration coupling, i.e., $\lambda = 0.1\epsilon_0$ and $\lambda = 0.2\epsilon_0$. We observe initially a strong increase of the cooling rate with increasing ξ. For $\xi \gtrsim 0.1$, however, the cooling rate saturates.

The initial and the asymptotic effective vibrational temperatures as a function of the lead temperature T are shown in Fig. 5(b). For the depicted temperature range, the initial temperature T_{init} exceeds the steady-state value T_{ph}, thus, maintaining the cooling effect for a range of lead temperatures of at least one order of magnitude. We also observe that T_{init} is not directly proportional to the lead temperature which originates from the preparation of our initial state which includes all couplings.

Conclusion.—We have established a simple model to illustrate the principle of cooling a magnetic nanoisland by a spin-polarized charge current. It is based on the polarization of the island magnetization by the flowing polarized electron spins and a subsequent removal of thermal energy from the vibration via a magnetomechanical coupling. Interestingly, this coupling also overcompensates Ohmic heating and leads to a significant lowering of the energy stored in the vibration. We also have found that the cooling rate saturates as a function of the magnetomechanical coupling, implying that not very strong couplings are

required to observe the proposed effect. We are confident that this mechanism could be realized in magnetic molecular nanojunctions by present-day technology.

We acknowledge financial support by the DFG via the Schwerpunktprogramm Spin Caloric Transport (Grant No. SPP 1538). P. N. thanks the BSH Bosch und Siemens Hausgeräte GmbH for interesting and useful insights into cooling technology.

[1] F. Giazotto, T. T. Heikkilä, A. Luukanen, A. M. Savin, and J. P. Pekola, Rev. Mod. Phys. **78**, 217 (2006); J. T. Muhonen, M. Meschke, and J. P. Pekola, Rep. Prog. Phys. **75**, 046501 (2012).
[2] F. Pobell, *Matter and Methods at Low Temperatures* (Springer, Berlin, 2007).
[3] J. König and J. Martinek, Phys. Rev. Lett. **90**, 166602 (2003).
[4] K. Flensberg, Phys. Rev. B **68**, 205323 (2003).
[5] S. Braig and K. Flensberg, Phys. Rev. B **68**, 205324 (2003).
[6] J. Koch, M. Semmelhack, F. von Oppen, and A. Nitzan, Phys. Rev. B **73**, 155306 (2006).
[7] A. L. Efros, M. Rosen, and E. I. Rashba, Phys. Rev. Lett. **87**, 206601 (2001).
[8] B. Sothmann and J. König, Phys. Rev. B **82**, 245319 (2010).
[9] M. M. E. Baumgärtel, M. Hell, S. Das, and M. R. Wegewijs, Phys. Rev. Lett. **107**, 087202 (2011).
[10] J. P. Launay and M. Verdaguer, *Electrons in Molecules: From Basics Principles to Molecular Electronics* (Oxford University Press, Oxford, 2013).
[11] J. König, H. Schoeller, and G. Schön, Phys. Rev. Lett. **76**, 1715 (1996).
[12] J. König, J. Schmid, H. Schoeller, and G. Schön, Phys. Rev. B **54**, 16820 (1996).
[13] I. Bargatin and M. L. Roukes, Phys. Rev. Lett. **91**, 138302 (2003).
[14] P. Rabl, P. Cappellaro, M. V. Gurudev Dutt, L. Jiang, J. R. Maze, and M. D. Lukin, Phys. Rev. B **79**, 041302 (2009).
[15] A. A. Kovalev, L. X. Hayden, G. E. W. Bauer, and Y. Tserkovnyak, Phys. Rev. Lett. **106**, 147203 (2011).
[16] A. Pályi, P. R. Struck, M. Rudner, K. Flensberg, and G. Burkard, Phys. Rev. Lett. **108**, 206811 (2012).
[17] D. Rugar, R. Budakian, H. J. Mamin, and B. W. Chui, Nature (London) **430**, 329 (2004).
[18] O. Arcizet, V. Jacques, A. Siria, P. Poncharal, P. Vincent, and S. Seidelin, Nat. Phys. **7**, 879 (2011).
[19] S. Kolkowitz, A. C. Bleszynski Jayich, Q. P. Unterreithmeier, S. D. Bennett, P. Rabl, J. G. E. Harris, and M. D. Lukin, Science **335**, 1603 (2012).
[20] M. Ganzhorn, S. Klyatskaya, M. Ruben, and W. Wernsdorfer, Nat. Nanotechnol. **8**, 165 (2013).
[21] Electron-spin vibration interactions are absorbed in the effective spin-independent electron-vibration coupling λ and do not induce spin flips along with vibrational relaxation in our model.
[22] The results do not change significantly when the various interacting terms are included in this definition.